ChemComm

Accepted Manuscript

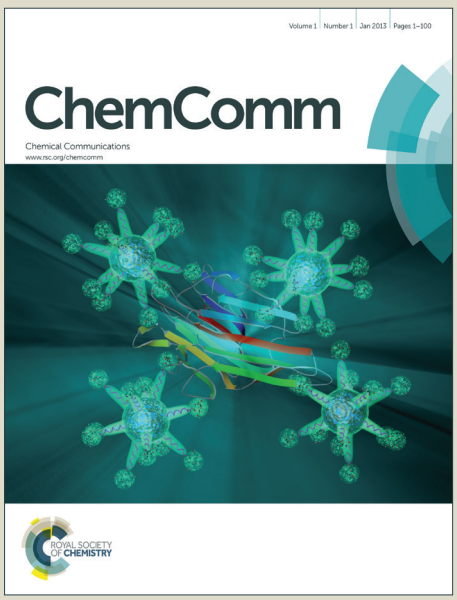

ROYAL SOCIETY OF CHEMISTRY

www.rsc.org/chemcomm

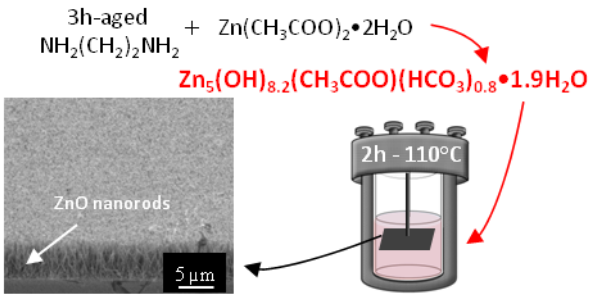

A new zinc hydroxy acetate hydrogen carbonate lamellar phase leads to clean and well crystallized ZnO nanorods.

Cite this: DOI: 10.1039/c0xx00000x

www.rsc.org/xxxxxx

ARTICLE TYPE

A new zinc hydroxy acetate hydrogen carbonate lamellar phase for growing large and clean ZnO nanorods arrays

Laurent Schlur[a], Anne Carton[a], Geneviève Pourroy[a]*

Received (in XXX, XXX) Xth XXXXXXXXX 20XX, Accepted Xth XXXXXXXXX 20XX

DOI: 10.1039/b000000

A novel zinc hydroxy acetate hydrogen carbonate $Zn_5(OH)_{8.2}(CH_3COO)(HCO_3)_{0.8}$•$1.9H_2O$, isomorphous to $Zn_5(OH)_8(CH_3COO)_2$,xH_2O, has been obtained upon reaction of zinc acetate dihydrate in aged ethylenediamine. This phase allows the growth on a substrate of large arrays of oriented and crystallized nanorods up to 8 µm in length, without crystallization of additional particles.

One-dimensional (1D) inorganic nanostructures such as nanorods, nanowires, nanotubes have attracted great attention due to their significance in basic scientific research and potential technological applications.[1] The high surface-to-volume ratio, the efficient electron transport properties as well as the good chemical and thermal behaviour of these structures, make them interesting for various fields of application, ranging from catalysis[2] or over sensors,[3] to electronics[4] and optoelectronics.[5,6]

Zinc oxide has been one of the most studied 1D nanostructured materials over the last years because of its direct wide band gap of 3.37 eV, a large exciton binding energy of 60 meV at room temperature and piezoresistive properties.[7] ZnO 1D nanostructures can be used for several applications such as solar cells,[6,9] sensors,[10] photocatalysts,[11] and field emission devices.[12] They are grown on substrates either using vapour phase syntheses or in solutions.[8] The former requires expensive equipment, high temperatures and time-consuming procedures,[13] whereas the latter is easy to perform, at low temperatures, compatible with flexible and vulnerable substrates.[14] Recent studies point out the growing interest in large arrays of ZnO single-crystalline nanorods for photovoltaic applications.[6,9] Most of the time, they are obtained at low temperatures (about 90°C) by reaction of zinc nitrate hexahydrate ($Zn(NO_3)_2$•$6H_2O$) in methenamine (hexamethylenetetramine $C_6H_{12}N_4$) aqueous solution.[15]

In a previous work, we used a zinc acetate dihydrate ($Zn(CH_3COO)_2$•$2H_2O$) and ethylenediamine (EDA) solution. to grow single-crystalline ZnO nanorods arrays, well oriented, having very few structural defects[16] and tuneable length from 1 to 8 µm.[6] Ethylenediamine and zinc acetate dihydrate have the advantage to avoid any incorporation of cations or anions such as Na^+, K^+ or nitrate. We showed that $Zn_5(OH)_8(CH_3COO)_2$•xH_2O is formed immediately after the reactant mixing and acts during the reaction, as a kind of reservoir for the growth of the rods on the substrate but also induced the growth of micrometric ZnO particles in the solution. These particles can fix on the top of the nanorods array, that is detrimental for the performances of ZnO nanorods devices. In hybrid solar cells, impurities on the top of nanorods lead to the apparition of short circuits and consequently to a decrease of efficiency.[6] In this study, we show that ageing the EDA solution before use leads to a new intermediate hybrid phase, more stable during the hydrothermal synthesis and avoiding impurities nucleation.

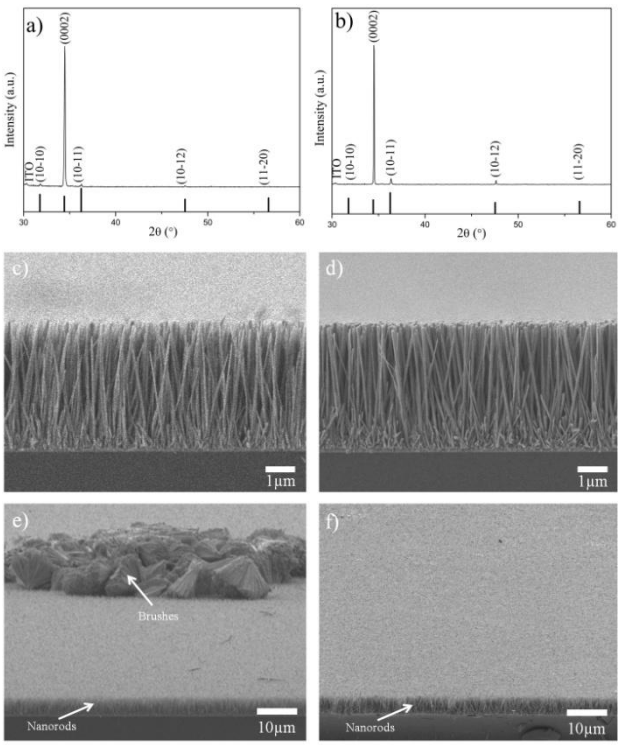

Fig.1 Typical X-rays diffraction patterns recorded on the substrate after hydrothermal treatment with fresh (a) and 3 h-aged EDA (b), Miller indices and diffraction lines corresponding to ZnO wurtzite (JCPDS card n°36-1451 (a and b); SEM images of the nanorods grown on the indium tin oxide ITO substrate with fresh EDA (c and e) and with 3h-aged EDA (d and f). The samples are titled 85° down in e) and f) images.

ZnO nanorods were grown on a ZnO seeds-coated indium tin oxide (ITO) substrate in a hydrothermal solution containing zinc acetate dihydrate and ethylenediamine (EDA). Zinc acetate dihydrate ($Zn(CH_3COO)_2$•$2H_2O$, 98%) and EDA ($C_2H_4(NH_2)_2$, ≥99%) were purchased from Alfa Aesar and Sigma-Aldrich, respectively. Indium tin oxide (ITO) (≤ 20 Ω/square) coated glass substrate was purchased from Precision Glass Optics. The ZnO

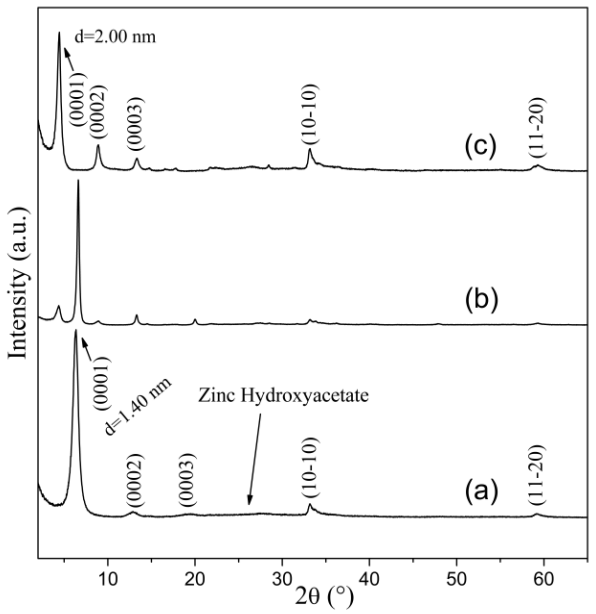

Fig.2. Diffractograms recorded on the precipitate obtained by mixing ethylenediamine (EDA) with zinc acetate dihydrate for EDA freshly prepared (a), after 1 h ageing (b) and 3 h ageing (c).

seeds layer was deposited on the ITO substrate according to Schlur et al.[6]. ZnO nanorods were grown under hydrothermal treatment. In a typical procedure, 10 mL of an aqueous solution of EDA (20 vol. %) aged either 0 min, or 1 h, or 3 h under air was mixed with 24 mL of an aqueous $Zn(CH_3COO)_2•2H_2O$ (0.72 M) solution. This prepared solution was then poured into a home-made Teflon lined stainless autoclave (V = 110 mL). The seeds-coated substrate was suspended horizontally upside-down in the autoclave. The later is heated at 110°C during 2 hours, then washed with water and dried 10 min at 50°C in air.

X-ray diffraction (XRD) patterns were collected on a Siemens D5000 diffractometer equipped with a quartz monochromator and Cu Kα1 radiation (λ=0.154056 nm). After the hydrothermal synthesis, the XRD pattern of the substrate exhibits ZnO diffraction lines with a strong preferential orientation in (002) lattice dimension (Fig. 1a and 1b). Images of ZnO nanorods obtained with a scanning electron microscope (SEM) JEOL 6700 are shown in Fig. 1c to 1f. Fig. 1a, 1c, 1e and Fig. 1b, 1d, 1f correspond to the nanorods synthesized with fresh and 3h-aged EDA respectively. In the two cases, nanorods of several microns in length have grown on the seeds layer. Whatever the EDA ageing time, the nanorods are oriented perpendicularly to the substrate. The nanorods length and diameter are homogeneous, respectively 4.05 ± 0.12 μm and 96 ± 17 nm for the fresh EDA, and 4.01 ± 0.11 μm and 99 ± 25 nm for the 3h-old EDA. The difference between the samples is visible when looking at the top of nanorods. Micronic particles having a brush shape are observed on the top surface when EDA is not aged before use (Fig. 1e), whereas nothing but the nanorods are present when EDA is aged 3h (Fig. 1f).

In order to determine the factor leading to the crystallization of extra brushes, we studied the phases formed during the process.

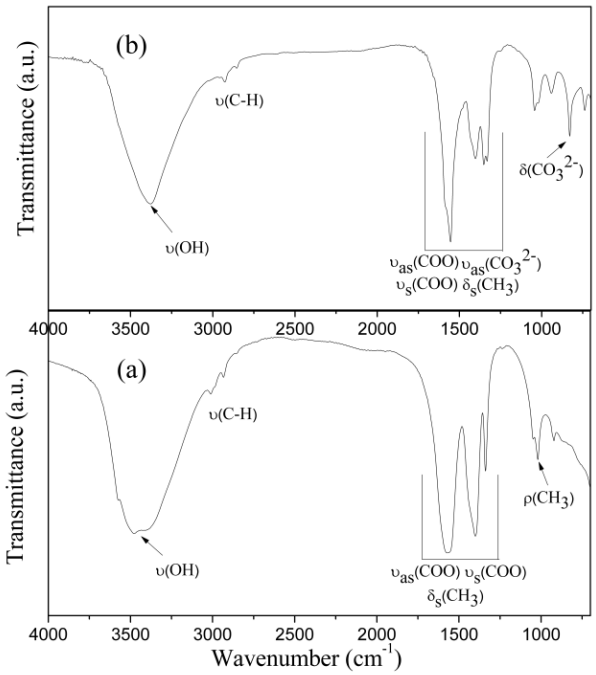

Fig.3 FTIR spectra of the precipitates obtained by mixing fresh EDA (a) or 3 h aged EDA (b) with zinc acetate dihydrate.

When EDA is mixed with zinc acetate dihydrate, a precipitate is formed immediately in the solution. The precipitates for the 3 ageing times have been washed three times in distilled water by centrifugation and dried, then characterized by the combined use of XRD, thermogravimetry analysis (TGA), Fourier Transformed Infrared spectroscopy (FTIR) and elemental analysis ICP-AES. The XRD patterns are presented in Fig. 2. When freshly prepared EDA is used (Fig. 2a), the pattern can be indexed in the hexagonal system of the well known zinc hydroxy acetate $Zn_5(OH)_8(CH_3COO)_2•nH_2O$.[17,18] This hybrid structure can be described as triple deck of inorganic layers $[Zn_5(OH)_8(H_2O)_n]^{2+}$separated by acetate anions.[19] This triple layer is formed of a monolayer of octahedral Zn^{II} hydroxide with metal vacancies counter-balanced by tetrahedral Zn^{II} sites on both sides of the octahedral monolayer. For 3h-ageing time (Fig. 2c), another phase which looks close to the previous one is formed. For intermediate ageing time, i.e. 1h in Fig. 2b, the two phases are observed. The position of the (10-10) and (11-20) diffraction peaks is the same for the two phases. Only (000l) peaks are shifted to lower angles when EDA is aged. It can be concluded that their respective layers have the same $[Zn_5(OH)_8(H_2O)_n]^{2+}$ structural unit, but with different interlayer distances. The interlayer distance calculated from the (0001) peak position is equal to 1.40 nm for freshly prepared EDA and to 2.00 nm for 3 h-ageing EDA. That has to be compared with 1.34 nm, characteristic of the ideal zinc hydroxy acetate ($Zn_5(OH)_8(CH_3COO)_2•2H_2O$) interlayer distance.[17] In such compounds, the increase of the interlayer distance is known to be due to various amounts of molecules between the layers.[18]

Fourier Transformed Infra Red (FTIR) spectroscopy has been performed on both hybrid lamellar phases using a Digilab FTS 3000 computer-driven instrument in transmittance with a

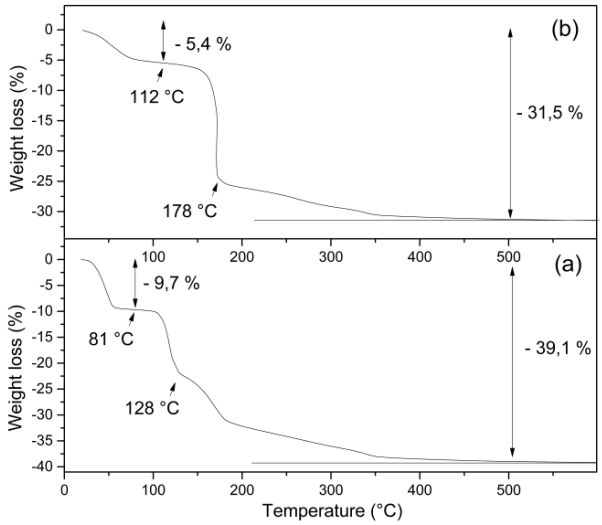

Fig.4 Thermogravimetric analysis of the precipitate obtained immediately after mixing fresh EDA (a) or 3 h-aged EDA (b) with zinc acetate dihydrate.

resolution of 4 cm^{-1} (Powder sample ca. 1% in KBr) (Fig. 3). The interlayer acetate anions are clearly detected in the precipitate formed with fresh EDA.[18] Indeed, the bands at ca. 2900 cm^{-1} can be attributed to the υ(C-H) stretching vibrations and the bands at 1566 and 1398 cm^{-1} are due to the antisymmetric and symmetric vibrations of the carboxylate groups. Concerning the phase with the bigger interlayer (Fig. 3c), the band at 830 cm^{-1} can be attributed to the bending mode $\delta(CO_3^{2-})$ of carbonates groups.[21] Knowing that this phase precipitates only after an exposure of EDA to air, it can be assumed that carbonates come from the well known reaction between CO_2 and EDA according to the reaction:[20]

$$2\ CO_2 + 2\ H_2O + H_2N(CH_2)_2NH_2 \leftrightarrow {}^{+}H_3N(CH_2)_2NH_3^{+} + 2\ HCO_3^{-} \quad \text{(eq. 1)}$$

The pH of the hydrothermal solution is equal to 8.2, and HCO_3^- is probably the carbonate form present in solution. Two vibrations modes at 2926 cm^{-1} and 2855 cm^{-1} associated to the symmetric and antisymmetric stretchings of the ν(C-H) bonds are also visible. They prove that acetates can be found in the phase obtained with aged EDA.

TGA were performed by means of a Texas Instrument SDT Q600 apparatus at a heating rate of 2°C/min in air. The precipitate formed with fresh EDA exhibits a thermal behaviour close to $Zn_5(OH)_8(CH_3COO)_2 \cdot 2H_2O$.[22] A first weight loss of 9.7 % is due to the evaporation of water (Fig. 4a). The loss observed above 81°C can be attributed to the condensation of hydroxyl groups. The last reaction above 128°C corresponds to the decomposition of the acetates. Finally, ZnO is obtained and the total mass loss is 39.1%. The decomposition in air of the precipitate obtained with the 3 h-aged EDA is slightly different. A first loss of mass of 5.4% due to the evaporation of water is visible on the thermogram (Fig. 4b). The two other mass losses at 112°C and 178°C are due to the condensation of the hydroxyl groups and the decomposition of the organic part of the compound. The final compound is identified by XRD as being ZnO after a total loss of 31.5%.

According to the elemental analyses performed at the Service Central d'Analyse CNRS (USR59) and given with a standard deviation of 0.5%, the composition of the precipitate obtained

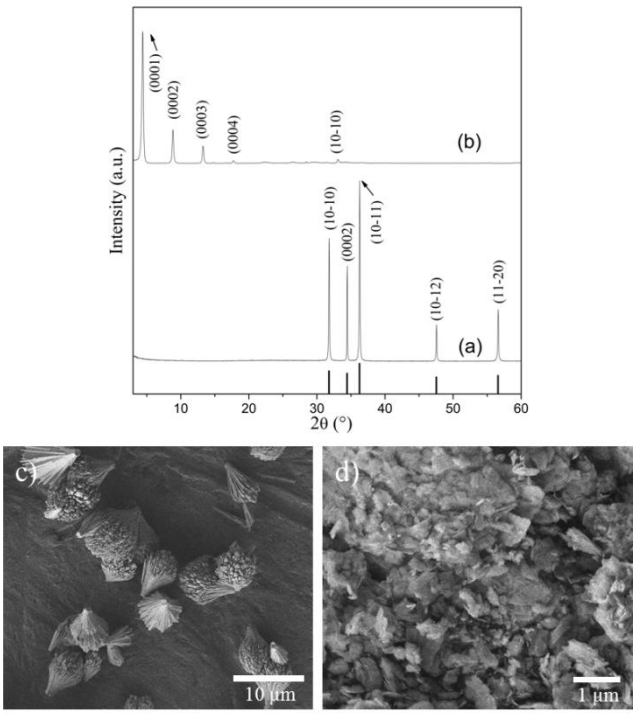

Fig.5 X-rays diffraction pattern (a-b) and SEM images (c-d) of the precipitates present in the autoclave at the end of the synthesis. The synthesis was performed with fresh EDA (a and c) or 3 hours aged EDA (b and d). Miller indices in the zinc hydroxyacetate space group (a) and according to ZnO wurtzite JCPDS card n°36-1451 (b).

with freshly prepared EDA is: Zn: 49.2 wt. %, C: 8.69 wt.%, H: 2.84 wt.%. The chemical formula calculated from these values is $Zn_5(OH)_{7.6}(CH_3COO)_{2.4} \cdot 3.7H_2O$. This formula for which the decomposition into ZnO corresponds to a mass loss of 38.8% is in agreement with the weight loss (39.1%) observed by thermogravimetric analysis. Acetate and water are in excess with respect to the theoretical formula ($Zn_5(OH)_8(CH_3COO)_2 \cdot 2H_2O$), resulting in highest interlayer distances. The chemical composition of the other phase (with the 3 h-aged EDA) is different. The elemental analysis of that compound gives Zn: 52.0 wt.%, C: 6.79wt.%, H: 2.26 wt.% and N: 0.15 wt.%. It confirms that no EDA derivatives are present in the unidentified hybrid material, because the nitrogen percentage is too low. According to FTIR spectroscopy and elemental analysis, the chemical formula is written $Zn_5(OH)_{8.2}(CH_3COO)(HCO_3)_{0.8} \cdot 1.9H_2O$. A complete decomposition into ZnO leads to a weight loss of 33% close to the 31.5 % observed by TGA.

So finally, the compounds obtained immediately after mixing fresh or 3 h-aged EDA with zinc acetate dihydrate are $Zn_5(OH)_{7.6}(CH_3COO)_{2.4} \cdot 3.7H_2O$ and $Zn_5(OH)_{8.2}(CH_3COO)(HCO_3)_{0.8} \cdot 1.9H_2O$ respectively. The former is less stable than the latter, since it decomposes at a lower temperature, 81°C for $Zn_5(OH)_{7.6}(CH_3COO)_{2.4} \cdot 3.7H_2O$ and 112°C for $Zn_5(OH)_{8.2}(CH_3COO)(HCO_3)_{0.8} \cdot 1.9H_2O$ (Fig. 4).

After 2 hours of reaction at 110°C, the precipitates remaining in the bottom of the autoclave have been characterized by XRD and SEM (Fig. 5). The two compounds look quite different. In the case of fresh EDA, SEM images exhibit brushes already observed on Fig. 1e at the top of nanorods. The XRD confirms that all the starting precipitate has been transformed into ZnO in agreement

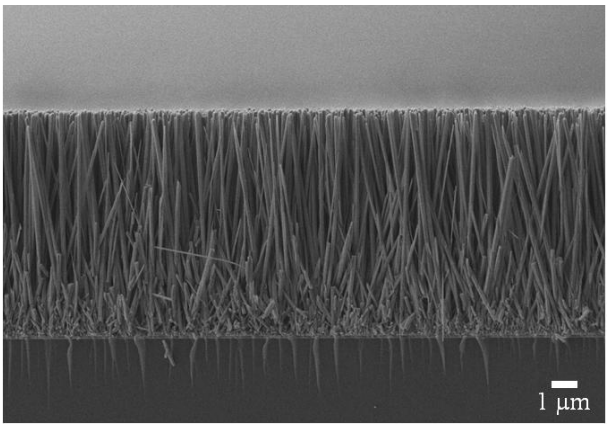

Fig.6 SEM side view of the nanorods obtained with 3h-aged EDA and with a hydrothermal solution two times more concentrated.

with TGA showing that the decomposition occurs above 81 °C. This decomposition provides nucleation sites for the growth of ZnO brushes into the hydrothermal solution. On the contrary, the diffraction peaks of the zinc hydroxy acetate hydrogen carbonate lamellar phase are observed on XRD pattern in the case of 3h-ageing EDA (Fig. 5b). This phase has not decomposed which confirms the better thermal stability already observed previously by TGA. The platelet shapes observed on SEM images are consistent with the hybrid lamellar structure (Fig. 5d). The absence of ZnO brushes on the top of nanorods when EDA is aged (Fig. 1f) is due to the fact that no ZnO is formed in the hydrothermal solution after 2 hours of reaction at 110°C.

Ageing EDA prevents the formation of brushes, while nanorods of 5.3 µm in length can grow. The length is increased up to 8.3 µm when the concentration of reactants is doubled (Fig. 6) and always without formation of brushes.

In conclusion, we show a new way to obtain very clean ZnO nanorods arrays having very homogenous length, diameter and orientation, thanks to the hybrid lamellar reaction intermediate: $Zn_5(OH)_{8.2}(CH_3COO)(HCO_3)_{0.8}•1.9H_2O$, which is very stable in solution at 110°C. Tuning the concentration of the reactants permits easily to tune the length of the rods and to obtain longer nanorods.

The authors acknowledge the Région Alsace for financial support.

Notes and references

[a] *IPCMS-CNRS-Université de Strasbourg UMR 7504, 23 rue du Loess, BP 43, 67034 Strasbourg Cedex 2. Fax: +33 388 10 72 28; Tel: +33 388 10 71 34; E-mail: pourroy@ipcms.unistra.fr*

1 T. Zhai, L. Li, Y. Ma, M. Liao, Xi Wang, X. Fang, J. Yao, Y. Bando and D. Golberg, *Chem. Soc. Rev.*, 2011, **40**, 2986; S. A. Fortuna and X. Li, *Semicond. Sci. Technol.*, 2010, **25**, 024005.

2 K. Gong, F. Du, Z. Xia, M. Durstock and L. Dai, *Science*, 2009, **323**, 760.

3 D. Spitzer, D. Cotineau, N. Piazzon, S. Josset, F. Schnell, S. N. Pronkin, E. R. Savinova and V. Keller, *Angew. Chem. Int. Ed.*, 2012, **51**, 5334; W. J. Park, M. H. Kim, B. H. Koo, W. J. Choi, J.-L. Lee and J. M. Baik, *Sensors and Actuators B : Chemical*, 2013, **185**, 10.

4 J. Li, C. Papadopoulos, J. M. Xu and M. Moskovits, *Applied Physics Letters*, 1999, **75**, 367; S. Park, M. Vosquerichian and Z. Bao, *Nanoscale*, 2013, **5**, 1727-1752.

5 J. Wang and Z. Lin, *Chemistry of Materials*, 2010, **22**, 579; M. Klaumünzer, A. Kahnt, A. Burger, M. Mackovic, C. Münzel, R. Srikantharajah, E. Spiecker, A. Hirsch and W. Peukert, *Applied Materials & Interfaces*, 2014, **6**, 6724

6 L. Schlur, A. Carton, P. Lévêque, D. Guillon and G. Pourroy, *Journal Phys. Chem. C*, 2013, **117**, 2993.

7 S.Xu and Z.L. Wang, *Nano Res.*, 2011, **4**, 1013;

8 B. Weintraub, Z. Zhou, Y. Li and Y. Deng, *Nanoscale*, 2010, **2**, 1573.

9 D.-Y. Son, J.-H. Im, H.-S. Kim and N.-G. Park, *J. Phys. Chem. C*, 2014, **118**, 16567.

10 J. X. Wang, X. W. Sul, Y. Yang, H. Huang, Y. C. Lee, O. K. Tan and L. Vayssieres, *Nanotechnology*, 2006, **17**, 4995; H. T. Wang, B. S. Kang, F. Ren, L. C. Tien, P. W. Sadik, D. P. Norton, S.J. Pearton and J. Lin, *Applied Physics Letters*, 2005, **86**, 243503.

11 T. Sun, J. Qiu and C. Liang, *J. Phys. Chem. C*, 2008, **112**, 715.

12 B. Weintraub, S. Chang, S. Singamaneni, W. H. Han, Y. J. Choi, J. Bae, M. Kirkham, V. V. Tsukruk and Y. Deng, *Nanotechnology*, 2008, **19**, 435302.

13 Y. Zhang, R. E. Russo and S. S. Mao, *Applied Physics Letters*, 2005, **87**, 043106; M. Skompska and K. Zarebska, *Electrochimica Acta*, 2014, **127**, 467.

14 S.Baruah and J. Dutta, *Sci. Technol. Adv. Mater.*, 2009, **10**, 0130001.

15 L.Vayssieres, K. Keis, S.-E. Lindquist and A. Hagfeldt, *J. Phys. Chem. B*, 2001, **105**, 3350; S.Baruah and J. Dutta, *J. Crystal Growth*, 2009, **311**, 2549; N. O. V. Plank, I. Howard, A. Rao, M. W. B. Wilson, C. Ducati, R. S. Mane, J. S. Bendall, R. R. M. Louca, N. C. Greenham and H. Miura, *J. Phys. Chem. C*, 2009, **113**, 18515; Z. Liang, R. Gao, J.-L. Lan, O. Wiranwetchayan, Q. Zhang, C. Li and G. Cao, *Solar Energy Materials & Solar Cells*, 2013,**117**, 34.

16 A. Kovalenko, G. Pourroy, O. Crégut, M. Gallart, B. Honerlage and P. Gilliot, *J. Phys. Chem. C*, 2010, **114**, 9498.

17 E. Hosono, S. Fujihara, T. Kimura and H. Imai, *Journal of Colloid and Interface Science*, 2004, **272**, 391.

18 T. Biswick, W. Jones, A. Pacula, E. Serwicka and J. Podobinski, *Solid State Science*, 2009, **11**, 330.

19 L. Poul, N. Jouini and F. Fiévet, *Chem. Mater.*, 2000, **12**, 3123.

20 F. Zheng, D. N. Tran, B. J. Busche, G. E. Fryxell, R. S. Addleman, T. S. Zemanian, and C. L. Aardahl, *Industrial & Engineering Chemistry Research*, 2005, **44**, 3099.

21 M. Bucca, M. Dietzel, J. Tang, A. Leis and S. J. Köhler, *Chemical Geology*, 2009, **266**, 143

22 E. Kandare and J.M. Hossenlopp, *Inorg. Chem.* 2006, **45**, 3766

